Journal of Magnetic Resonance 214 (2012) 184–188

Contents lists available at SciVerse ScienceDirect

Journal of Magnetic Resonance

journal homepage: www.elsevier.com/locate/jmr

Use of Carr–Purcell pulse sequence with low refocusing flip angle to measure T_1 and T_2 in a single experiment

Fabiana Diuk de Andrade [a], Antonio Marchi Netto [b], Luiz Alberto Colnago [c,*]

[a] Instituto de Química de São Carlos, Universidade de São Paulo, Av. Trabalhador São-carlense 400, São Carlos, SP 13560-970, Brazil
[b] Instituto de Física de São Carlos, Universidade de São Paulo, Av. Trabalhador São-carlense 400, São Carlos, SP 13560-970, Brazil
[c] Embrapa Instrumentação, Rua XV de Novembro 1452, São Carlos, SP 13560-970, Brazil

ARTICLE INFO

Article history:
Received 20 June 2011
Revised 24 October 2011
Available online 17 November 2011

Keywords:
Carr–Purcell
CWFP
SSFP
Relaxation time
Time domain NMR

ABSTRACT

The Carr–Purcell pulse sequence, with low refocusing flip angle, produces echoes midway between refocusing pulses that decay to a minimum value dependent on T_2^*. When the refocusing flip angle was $\pi/2$ (CP_{90}) and $\tau > T_2^*$, the signal after the minimum value, increased to reach a steady-state free precession regime (SSFP), composed of a free induction decay signal after each pulse and an echo, before the next pulse. When $\tau < T_2^*$, the signal increased from the minimum value to the steady-state regime with a time constant $(T^*) = 2T_1T_2/(T_1 + T_2)$, identical to the time constant observed in the SSFP sequence, known as the continuous wave free precession (CWFP). The steady-state amplitude obtained with $M_{CP90} = M_0T_2/(T_1 + T_2)$ was identical to CWFP. Therefore, this sequence was named CP-CWFP because it is a Carr–Purcell sequence that produces results similar to the CWFP. However, CP-CWFP is a better sequence for measuring the longitudinal and transverse relaxation times in single scan, when the sample exhibits $T_1 \sim T_2$. Therefore, this sequence can be a useful method in time domain NMR and can be widely used in the agriculture, food and petrochemical industries because those samples tend to have similar relaxation times in low magnetic fields.

1. Introduction

The Carr–Purcell pulse sequence (CP) is based on the spin-echo sequence introduced by Hahn in 1950 to measure the transverse relaxation time, T_2 [1]. The Hahn sequence uses two $\pi/2$ pulses separated by a time interval (τ), where $T_2^* \ll \tau < T_2$. Hahn had observed that this sequence was sensitive to molecular diffusion through the inhomogeneous magnetic field. To solve the effect of diffusion in the T_2 measurement, Carr and Purcell [2] introduced a pulse sequence that used a $\pi/2$ excitation pulse, followed by a train of π refocusing pulses using the same phase of the excitation pulse. The time interval between the refocusing pulses was doubled compared to time between the excitation and the first refocusing pulse. This sequence produced echoes with a maximum amplitude midway through the refocusing pulses. Each echo was dephased by 180° from the preceding echo. This sequence used a small τ value between the refocusing pulses, which minimized the effect of diffusion in the echoes' signals. However, Meiboom and Gill [3] observed that the adjustment of π refocusing pulses was critical and this problem was more pronounced for samples with long T_2 (liquid) values and using an inhomogeneous magnet. Thus, it was necessary to use short values for τ and a large number of refocusing pulses to eliminate the effects of diffusion. A small deviation from the exact value of π was cumulative; thus, the error of the refocusing pulses increased with the number of pulses and introduced error in the T_2 measurements as a consequence. To solve this problem, Meiboom and Gill [3] proposed a modification to the CP sequence by introducing a 90° phase shift between the excitation and the refocusing pulses. This improvement made the sequence very robust and insensitive to error in the refocusing pulse. Therefore, the sequence proposed by Carr–Purcell and improved by Meiboom and Gill, known today as CPMG, is the standard method to measure T_2. This sequence is so robust that we have recently shown that it is possible to measure T_2 using very low refocusing flip angles, as low as $\pi/4$ [4]. The major advantage in using CPMG with low refocusing flip angles occurs when it is necessary to reduce the applied power, as in online measurement [4] or in fast imaging techniques, to reduce the power deposition in the samples.

In this paper, the effect of low refocusing flip angles in the CP pulse sequence is shown. The use of $\pi/2$ refocusing pulses produced signal similar to continuous wave free precession (CWFP), a special condition of the steady state free precession (SSFP) regime [6]. The sequence was named CP-CWFP because it is a CP sequence with $\pi/2$ pulses and produced results similar to CWFP. Therefore CP-CWFP sequence can have similar CWFP applications, e.g. be

* Corresponding author. Fax: +55 16 21072902.
E-mail addresses: fabianadiuk@yahoo.com.br (F.D. de Andrade), nettomarchi@gmail.com (A. Marchi Netto), colnago@cnpdia.embrapa.br (L.A. Colnago).

1090-7807/$ - see front matter © 2011 Elsevier Inc. All rights reserved.
doi:10.1016/j.jmr.2011.11.004

used to measure T_1 and T_2 in a single experiment. CP-CWFP sequence is less sensitive to signal-to-noise in measuring T_1 and T_2 in a single experiment compared to CWFP when T_2 is similar to T_1.

2. Experimental

The samples studied were deionized water, acetone, dimethyl sulfoxide (DMSO), soybean oil and castor bean seeds.

The CP sequence with $\pi/2$ refocusing pulse was $\pi/2_x - \tau/2 - (\pi/2_x - \tau)_n$ (Fig. 1).

The experiments at 9 MHz for ^{1}H were performed at 25 ± 0.5 °C on a SLK-1300 spectrometer (SpinLock, Córdoba, Argentina) based on 0.23 T Halbach magnet, using a 100 mm diameter probe. The sequence used a $\pi/2$ refocusing pulse width of 9.5 μs, τ = 0.3 ms, 5 KHz offset frequency equivalent to $\psi = 3\pi$, a recycle delay >5T_1 and 16 scans. For a good analysis of the signal composition for CP with $\pi/2$ pulse it was used τ = 3 ms ($\tau > T_2^*$). In this condition the sequence was named CP-SSFP due to be composed of a spin echo and steady state free precession (SSFP) signal.

The experiments at 85 MHz for ^{1}H were performed at 22 ± 1 °C using a CAT-100 transceiver (Tecmag, Houston) and a 2.1 T Oxford superconducting magnet (Oxford, UK). The sequence utilized a $\pi/2$ refocusing pulse width of 14 μs, τ = 0.3 ms, 5 KHz offset frequency equivalent to $\psi = 3\pi$, a recycle delay >5T_1 and 4 scans. T_2^* measured from FID was 1.2 ms and 13 ms for 9 and 85 MHz, respectively.

The T_1 and T_2 values were measured using the Inversion-Recovery sequence (IR) [7] and CPMG pulse sequences [3], respectively. The IR intervals varied from 0.15 s to 25 s for acetone, deionized water and DMSO and from 1×10^{-6} s to 2 s for soybean and castor bean seeds. The CPMG echo times were 500 us for acetone, deionized water and DMSO and 50 μs for soybean and castor bean seeds.

3. Results and discussion

3.1. CP with π/2 pulses

Fig. 2 shows the real component of the soybean oil signal at 9 MHz, obtained with a CP sequence using $\pi/2$ refocusing pulses (CP_{90}) and $\tau > T_2^*$. This figure shows the signal from the first echo to the signal after 500 pulses. The arrows (A–C) indicate three important regions of the CP_{90} signal. Arrow A points the spin echoes signals, which decreased to a minimum value. Arrow B indicates the increase of the signal to a steady-state value (arrow C). These features are better illustrated in the expansions presented in Fig. 3. Fig. 3A–C corresponds to the signals, from 0 to 0.016 s (2A), between 0.016–0.048 s (2B) and 0.640–0.660 s (2C), respectively.

Fig. 3A shows the real component of signal of the first eight echoes for the CP_{90} sequence. The first echo was stronger than the second one, as expected, but with the same phase. This was not observed in the conventional CP, which used π refocusing pulses. In conventional CP, each echo is 180° out of phase from the previous one. The third and fourth echoes have similar amplitudes and are 180° out of phase from the first and second echoes. The same pattern, 180° dephasing every two pulses, was observed up to

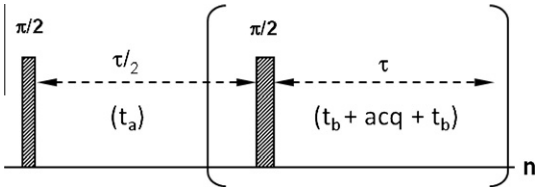

Fig. 1. Carr–Purcell sequence with $\pi/2$ refocusing pulses. When $\tau < T_2^*$: t_a = 144.5 μs, t_b = 67.25 μs and acq = 160 μs. When $\tau > T_2^*$: t_a = 1042.75 μs, t_b = 50 μs and acq = 2000 μs.

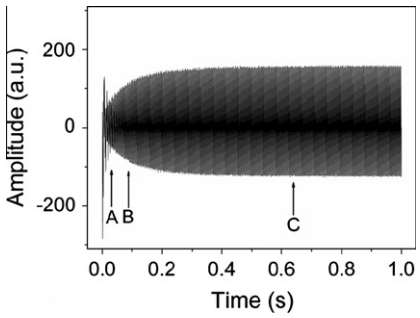

Fig. 2. Real components of the signal for the soybean oil sample obtained with CP sequence using $\pi/2$ refocusing pulses and $\tau > T_2^*$, from the first echo to the steady-state regime. The arrows A, B and C indicate three regions of the CP_{90} signal, which are expanded in Fig. 3.

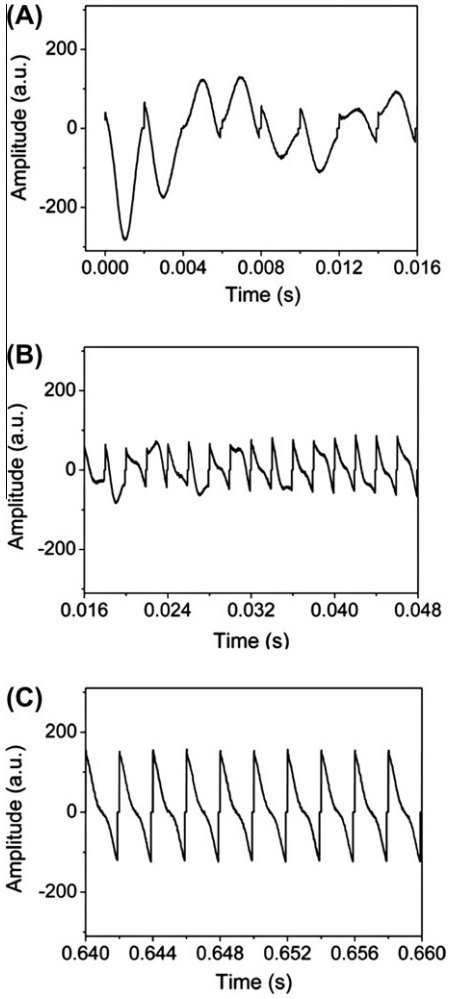

Fig. 3. Expansion of the real component of the signal for the soybean oil sample of Fig. 2. (A) 0–0.016 s, B) between 0.016–0.048 s and C) 0.640–0.660 s.

the eighth echo. However, the amplitudes of the last two even echoes were bigger than the respective odd echoes. The presence of the odd and even echoes with same phase occurred because it is necessary to use two $\pi/2$ pulses to invert the magnetization. When considering the $\pi/4$ pulse (data not shown), four pulses were necessary to invert the phase.

After the eighth pulse (Fig. 3B), the CP_{90} signals were not echoes and showed a complex signal up to approximately 0.048 s. After this time, the signal start to form a periodic pattern (Fig. 3C); it consisted of a positive signal that decayed to zero at the midway

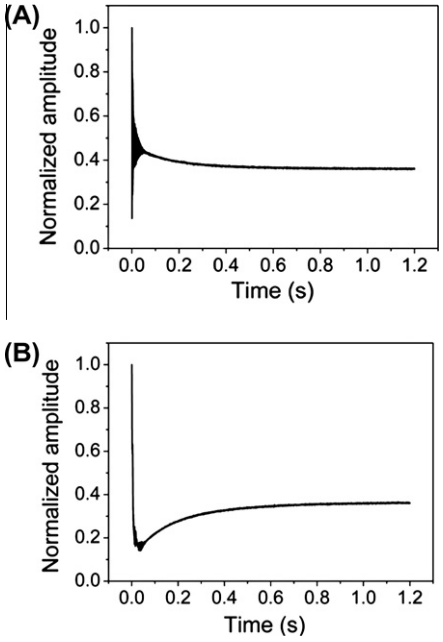

Fig. 4. CWFP (A) and CP-CWFP (B) signals of soybean oil acquired at 85 MHz, $T_1/T_2 \sim 2$.

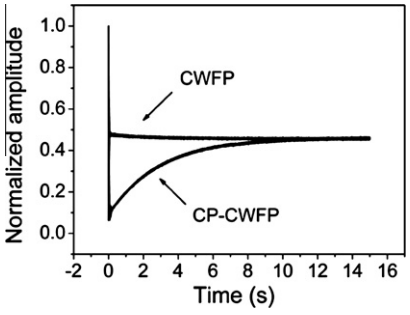

Fig. 5. CWFP and CP-CWFP signals of the water sample acquired at 85 MHz, $T_1/T_2 \sim 1$.

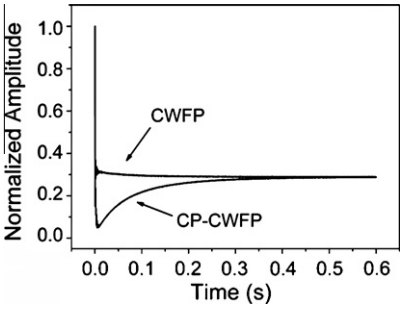

Fig. 6. CWFP and CP-CWFP signals of soybean oil acquired at 9 MHz, $T_1/T_2 \sim 1$.

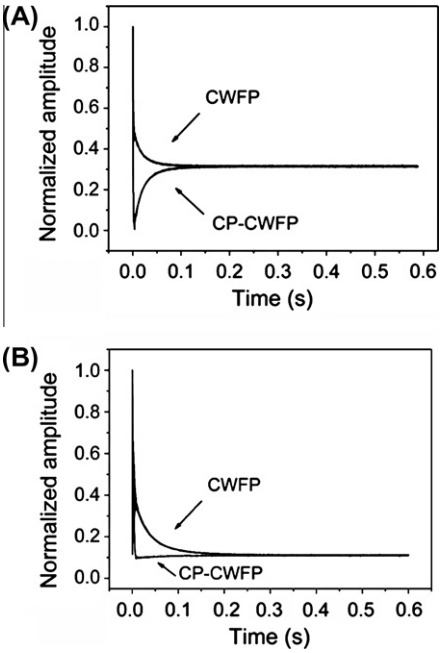

Fig. 7. CWFP and CP-CWFP signals of castor bean seeds acquired at (A) 9 MHz, $T_1/T_2 \sim 2$; and at (B) 85 MHz, $T_1/T_2 \sim 10$.

point between the refocusing pulses and became negative, reaching the minimum negative value before the next pulse. These signals increased and became more stable, reaching maximum amplitude at approximately 0.6 s (Fig. 2, arrow C and Fig. 3C). The signal in Fig. 3C was a typical SSFP signal, composed of a FID after each pulse and an echo before the next one [5]; this means that the complex signals in Fig. 3B were related to the transition between the echoes produced in the beginning of the sequence and the FID and echo signals at the end of the sequence.

The same type of signal has also been observed with other low values of the refocusing pulse (data not shown). Therefore, the CP sequence with $\pi/2$ pulses was composed of a spin echo and SSFP signals; thus, it was named the CP-SSFP sequence. Consequently, the sequence can have a similar application to the SSFP sequence, as do most of the signals produced by this sequence in this condition. When $\tau \ll T_2^*$, the SSFP sequence shows a special condition known as continuous wave free precession (CWFP) [6,8]; thus, the CP sequence with $\pi/2$ pulses using $\tau \ll T_2^*$ has been named CP-CWFP.

3.2. Comparison between CWFP and CP-CWFP pulse sequences

The CWFP regime is obtained when a train of pulses with same phase and amplitude, separated by a fixed time $\tau \ll T_2^* < T_2$, is applied to a sample. Fig. 4A shows the magnitude of a CWFP signal (soybean oil) from thermal equilibrium to the steady-state regime. This signal obtained with an offset frequency or precession angle $\psi = (2n+1)\pi$, where n is an integer and $\tau < 1/2T_2^*$, shows two transient regimes before reaching a constant steady state [6,8]. The first transient regime was characterized by an alternation of the signal amplitude between even and odd pulses [6,8,9]. The alternation of the signal after the odds pulses decays to an intermediate amplitude, governed by a time constant related to T_2^* [6,8]. The signal after the even pulses starts from the minimum value increased to the same value observed after the odd pulses. When the amplitudes of the signals after each of the even and odd pulses were similar, they reached the quasi-stationary state (QSS). After this time point, the signal exhibited a slower decay, controlled by T_1/T_2 and reached a steady state regime at approximately $5T^*$, where T^* is the time constant of the QSS decay. When the CWFP signal was produced by the train of $\pi/2$ pulses and $\psi = (2n+1)\pi$, T^* was dependent on the T_1 and T_2 provided by Eq. (1) [6] and the amplitude of the steady-state M_{CWFP} by Eq. (2). The CWFP signal of the soybean oil (Fig. 4A) has $T^* = 0.18$ s and $M_{CWFP} = 0.36$.

$$T^*_{(\alpha=\pi/2)} = \frac{2T_1T_2}{(T_1+T_2)} \quad (1)$$

Table 1
The relaxation times T_1 and T_2 of water, soybean oil and castor bean seed measured with IR and CMPG pulse sequences at 85 and 9 MHz.

Sample	ν (MHz ^{1}H)	T_1	T_2	T_1/T_2
Water	85	2.96 ± 0.05	2.45 ± 0.01	1.21
	9	2.73 ± 0.01	2.20 ± 0.01	1.24
Soybean oil	85	0.28 ± 0.01	0.14 ± 0.01	2.00
	9	0.12 ± 0.01	0.11 ± 0.01	1.09
Castor bean seed	85	0.16 ± 0.01	0.015 ± 0.001	10.67
	9	0.029 ± 0.001	0.014 ± 0.001	2.07

$$M_{\mathrm{CWFP}} = \frac{M_0 T_2}{(T_1 + T_2)} \tag{2}$$

The magnitude of the CP-CWFP signal for the same sample (Fig. 4B) showed some differences and similarities in the CWFP signal. The first difference was that the signal decayed to a minimum value after even and odd pulses; then, the signal increased to reach a steady-state regime.

Although CWFP and CP-CWFP have these differences, they share some identical properties. The signals from QSS in CWFP and the minimum amplitude in CP-CWFP reached a steady-state regime with the same time constant T^*. When the CP-CWFP signal was acquired using $\pi/2$ pulses and the precession angle $\psi = (2n+1)\pi$, T^* was governed by T_1 and T_2 (Eq. (1)) and T^* = 0.18 s identical to the one observed in the CWFP signal of the soybean oil (Fig. 4A). The CP-CWFP and CWFP showed an identical normalized steady-state amplitude $M_{\mathrm{CP\text{-}CWFP}}$ = 0.36, given by Eq. (2) (Fig. 4B).

Eqs. (1) and (2) can be rearranged to Eqs. (3) and (4) [6]. With these equations, the relaxation times T_1 and T_2 can be calculated from the time constant $T^*_{(\alpha=\pi/2)}$ and the normalized magnetization amplitude $M_{\mathrm{CP\text{-}CWFP}}/M_0$ or M_{CWFP} and thermal equilibrium (M_0). The amplitude of M_0 was assumed to be the intensity after the first pulse and M_{CWFP} or $M_{\mathrm{CP\text{-}CWFP}}$ after reaching a steady state. Therefore, the CP-CWFP sequence can also measure T_1 and T_2 in a single experiment, as CWFP [5].

$$T_1 = \frac{T^*_{(\alpha=\pi/2)}/2}{M_{\mathrm{CWFP}}/M_0} \tag{3}$$

$$T_2 = \frac{T^*_{(\alpha=\pi/2)}/2}{1 - M_{\mathrm{CWFP}}/M_0} \tag{4}$$

Figs. 5–7 show a comparison between CWFP and CP-CWFP for the samples with $T_1/T_2 \sim 1$ (water), $T_1/T_2 \sim 2$ (soybean oil) and $T_1/T_2 \sim 10$ (castor bean oil), using two magnetic fields at 0.23 T (9 MHz) and 2.1 T (85 MHz) with $T_2^* = 1.2$ and 13 ms, respectively. The T_1 and T_2 values for these three samples at 9 and 85 MHz were measured with IR and CMPG (Table 1).

Fig. 5 illustrates the advantages of CP-CWFP over CWFP to measure the relaxation times when $T_1 \sim T_2$. This Fig. 5 shows the measurement at 85 MHz, which was very similar to those measured at 9 MHz. When $T_1 \sim T_2$, the difference in amplitudes during the QSS in the CWFP signal was minimum, and the error for T^* measurement was more than 10%. Therefore, it was necessary to have a very high signal to noise ratio in the CWFP signal to have a good fit of T^*. Conversely, the difference in the amplitude during the QSS in CP-CWFP was the maximum and increased from the minimum value to the maximum amplitude of the steady-state signal, equivalent to $0.5M_0$. This large difference in the amplitudes made fitting T^* less dependent on the signal to noise ratio. Similar results are shown in Fig. 6 for soybean oil at 9 MHz with $T_1 \sim T_2$, in contrast to the same sample at 85 MHz with $T_1 \sim 2T_2$. Therefore, the CP-CWFP sequence is normally a better sequence than CWFP to measure the relaxation times in lower magnetic field spectrometers because T_1 and T_2 tend to have similar values. Therefore, the CP-CWFP sequence can be a more useful technique than CWFP to measure the relaxation times on low field NMR spectrometers, which are normally used in the agriculture and food industries [8,10–13] with $B_0 < 0.5$ T (20 MHz) and in the well logging NMR tools with $B_0 \sim 0.05$ T (2 MHz) [14].

When the samples exhibited values of $T_1 \sim 2T_2$, as soybean oil at 85 MHz (Fig. 4) or the castor bean seeds at 9 MHz (Fig. 7A), the CWFP and CP-CWFP had similar variations in the amplitude during the QSS decay. Therefore, both techniques could be used to calculate T^* and the relaxation times. Conversely, when $T_1 \gg T_2$, e.g., the castor bean seeds at 85 MHz with $T_1 \sim 11T_2$ (Fig. 7B), the CWFP had higher variations in the amplitude of the QSS decay compared to the CP-CWFP. Therefore, for a viscous sample at a high magnetic field and when $T_1 \gg T_2$, CWFP was a better option compared to CP-CWFP to measure the relaxation times.

4. Conclusion

The Carr–Purcell pulse sequence with $\pi/2$ pulses produced spin echoes signals which decays with T_2^*. Then the signal increase to reach a SSFP regime with a FID signal after the pulses and an echo before the pulse. When the sequence uses $\tau < T_2^*$, $\pi/2$ pulses and precession (ψ) in odd numbers of π, the signal showed several similarities to CWFP. Therefore, CP-CWFP can be used in the simultaneous measurements of T_1 and T_2 in a single scan, as CWFP. However, CP-CWFP has greater advantage over CWFP for samples with $T_1/T_2 \sim 1$. When $T_1/T_2 \sim 1$ the variation in the amplitude of CP-CWFP signal, during the QSS, was maximum. Conversely, the variation in the QSS amplitude in the CWFP signal was minimum. Therefore, the fitting of T^* in CP-CWFP is less sensitive to signal to noise ration than in the CWFP sequence.

Therefore, CP-CWFP is a better sequence compared to CWFP in the measurement of relaxation times in lower magnetic field spectrometers, where T_1 tends to have values similar to T_2. Therefore, the CP-CWFP sequence can be a useful method in low-field NMR spectrometry, which is widely used in the agriculture, food and petrochemical industries.

Acknowledgments

The authors wish to thank the FAPESP, CNPq and FINEP (Brazilian Agencies) for their financial support.

References

[1] E.L. Hahn, Spin echoes, Phys. Rev. 80 (1950) 580–594.
[2] H.Y. Carr, E.M. Purcell, Effects of diffusion on free precession in nuclear magnetic resonance experiments, Phys. Rev. 94 (1954) 630–638.
[3] S. Meiboom, D. Gill, Modified spin-echo method for measuring nuclear relaxation times, Rev. Sci. Instrum. 29 (1966) 93–102.
[4] F.D. de Andrade, A. Marchi Netto, L.A. Colnago, Qualitative analysis by *online* nuclear magnetic resonance using Carr–Purcell–Meiboom–Gill sequence with low refocusing flip angles, Talanta 84 (2011) 84–88.
[5] H.Y. Carr, Steady-state free precession in nuclear magnetic resonance, Phys. Rev. 112 (1958) 1693–1701.
[6] T. Venâncio, M. Engelsberg, R.B.V. Azeredo, N.E.R. Alem, L.A. Colnago, Fast and simultaneous measurement of longitudinal and transverse NMR relaxation

times in a single continuous wave free precession experiment, J. Magn. Reson. 173 (2005) 34–39.
[7] P.B. Kingsley, Methods of measuring spin–lattice (T_1) relaxation times: an annotated bibliography, Conc. Magn. Reson. 11 (1999) 243–276.
[8] C.C. Corrêa, L.A. Forato, L.A. Colnago, High-throughput non-destructive nuclear magnetic resonance method to measure intramuscular fat content in beef, Anal. Bioanal. Chem. 393 (2009) 1357–1360.
[9] R.B.V. Azeredo, L.A. Colnago, A.A. Souza, M. Engelsberg, Continuous wave free precession: a practical analytical tool for low resolution NMR measurements, Anal. Chim. Acta 478 (2003) 313–320.
[10] R.A. Prestes, L.A. Colnago, L.A. Forato, L. Vizzotto, E.H. Novotny, E. Carrilho, A rapid and automated low resolution NMR method to select intact oilseeds with a modified fatty acid profile, Anal. Chim. Acta 596 (2007) 325–329.
[11] F.Z. Ribeiro, L.V. Marconcini, I.B. Toledo, R.B.V. Azeredo, L.L. Barbosa, L.A. Colnago, Nuclear magnetic resonance water relaxation time chances in bananas during ripening: a new mechanism, J. Sci. Food Agric. 90 (2010) 2052–2057.
[12] L.A. Colnago, M. Engelsberg, A.A. Souza, L.L. Barbosa, High-throughput, non-destructive determination of oil content in intact seeds by continuous wave-free precession NMR, Anal. Chem. 79 (2007) 1271–1274.
[13] B.P. Hills, Applications of low-field NMR to food science, Annu. Rep. NMR Spectrosc. 58 (2006) 177–230.
[14] J. Mitchell, M.D. Hürlimann, E.J. Fordham, A rapid measurement of T_1/T_2: the DECPMG sequence, J. Magn. Reson. 200 (2009) 198–206.